



Engineering *Burkholderia xenovorans* LB400 BphA through Site-Directed Mutagenesis at Position 283

Junde Li,^{a,b,c} Jun Min,^{a,b,d} Yuan Wang,^{a,b,d} Weiwei Chen,^{a,b,c} Yachao Kong,^{a,b,c} Tianyu Guo,^a Jai Krishna Mahto,^e Michel Sylvestre,^f Xiaoke Hu^{a,b,d}

^aKey Laboratory of Coastal Biology and Bioresource Utilization, Yantai Institute of Coastal Zone Research, Chinese Academy of Sciences, Yantai, China

^bLaboratory for Marine Biology and Biotechnology, Qingdao National Laboratory for Marine Science and Technology, Qingdao, China

^cUniversity of Chinese Academy of Sciences, Beijing, China

^dCenter for Ocean Mega-Science, Chinese Academy of Sciences, Qingdao, China

^eDepartment of Biotechnology, Indian Institute of Technology Roorkee, Roorkee, Uttarakhand, India

^fInstitut National de la Recherche Scientifique (INRS–Institut Armand-Frappier), Laval, Québec, Canada

ABSTRACT Biphenyl dioxygenase (BPDO), which is a Rieske-type oxygenase (RO), catalyzes the initial dioxygenation of biphenyl and some polychlorinated biphenyls (PCBs). In order to enhance the degradation ability of BPDO in terms of a broader substrate range, the BphAE_{S283M}, BphAE_{p4-S283M}, and BphAE_{RR41-S283M} variants were created from the parent enzymes BphAE_{LB400}, BphAE_{p4}, and BphAE_{RR41}, respectively, by a substitution at one residue, Ser283Met. The results of steady-state kinetic parameters show that for biphenyl, the k_{cat}/K_m values of BphAE_{S283M}, BphAE_{p4-S283M}, and BphAE_{RR41-S283M} were significantly increased compared to those of their parent enzymes. Meanwhile, we determined the steady-state kinetics of BphAEs toward highly chlorinated biphenyls. The results suggested that the Ser283Met substitution enhanced the catalytic activity of BphAEs toward 2,3',4,4'-tetrachlorobiphenyl (2,3',4,4'-CB), 2,2',6,6'-tetrachlorobiphenyl (2,2',6,6'-CB), and 2,3',4,4',5-pentachlorobiphenyl (2,3',4,4',5-CB). We compared the catalytic reactions of BphAE_{LB400} and its variants toward 2,2'-dichlorobiphenyl (2,2'-CB), 2,5-dichlorobiphenyl (2,5-CB), and 2,6-dichlorobiphenyl (2,6-CB). The biochemical data indicate that the Ser283Met substitution alters the orientation of the substrate inside the catalytic site and, thereby, its site of hydroxylation, and this was confirmed by docking experiments. We also assessed the substrate ranges of BphAE_{LB400} and its variants with degradation activity. BphAE_{S283M} and BphAE_{p4-S283M} were clearly improved in oxidizing some of the 3-6-chlorinated biphenyls, which are generally very poorly oxidized by most dioxygenases. Collectively, the present work showed a significant effect of mutation Ser283Met on substrate specificity/regio-specificity in BPDO. These will certainly be meaningful elements for understanding the effect of the residue corresponding to position 283 in other Rieske oxygenase enzymes.

IMPORTANCE The segment from positions 280 to 283 in BphAEs is located at the entrance of the catalytic pocket, and it shows variation in conformation. In previous works, results have suggested but never proved that residue Ser283 of BphAE_{LB400} might play a role in substrate specificity. In the present paper, we found that the Ser283Met substitution significantly increased the specificity of the reaction of BphAE toward biphenyl, 2,3',4,4'-CB, 2,2',6,6'-CB, and 2,3',4,4',5-CB. Meanwhile, the Ser283Met substitution altered the regio-specificity of BphAE toward 2,2'-dichlorobiphenyl and 2,6-dichlorobiphenyl. Additionally, this substitution extended the range of PCBs metabolized by the mutated BphAE. BphAE_{S283M} and BphAE_{p4-S283M} were clearly improved in oxidizing some of the more highly chlorinated biphenyls (3 to 6 chlorines), which are generally very poorly oxidized by most dioxygenases. We used modeled and docked enzymes to identify some of the structural features that

Citation Li J, Min J, Wang Y, Chen W, Kong Y, Guo T, Mahto JK, Sylvestre M, Hu X. 2020. Engineering *Burkholderia xenovorans* LB400 BphA through site-directed mutagenesis at position 283. Appl Environ Microbiol 86: e01040-20. <https://doi.org/10.1128/AEM.01040-20>.

Editor Rebecca E. Parales, University of California, Davis

Copyright © 2020 American Society for Microbiology. All Rights Reserved.

Address correspondence to Xiaoke Hu, xkhu@yic.ac.cn.

Received 5 May 2020

Accepted 15 July 2020

Accepted manuscript posted online 24 July 2020

Published 17 September 2020

explain the new properties of the mutant enzymes. Altogether, the results of this study provide better insights into the mechanisms by which BPDO evolves to change and/or expand its substrate range and its regiospecificity.

KEYWORDS polychlorinated biphenyls, biphenyl dioxygenase, *Burkholderia xenovorans* LB400, substrate range, regiospecificity, enzyme mutation, enzyme catalysis, directed evolution

Polychlorinated biphenyls (PCBs) are a class of chlorinated derivatives of biphenyl that theoretically contain 209 congeners (1–4). Owing to the characteristics of PCBs, chemical durability, electrical insulating property, and incombustibility, numerous congeners of PCB have been utilized for many industrial applications (5, 6). A large amount of PCBs was manufactured, approximately 1.5 million tons, from 1929 to 1978 (7). Resulting from their hydrophobic properties, PCBs are persistent and have been evaluated to affect human health and ecosystems (8–12). PCBs have been designated toxic priority pollutants by the U.S. Agency for Toxic Substances and Disease Registry (ATSDR) (13, 14).

Several heterotrophic soil bacteria can use selected PCB congeners as sources of carbon and energy (15, 16). The enzymatic reactions involved in the PCB degradation process are organized into pathways (16–18). The ability of enzymes of these pathways to undergo a relaxation of their specificities toward a range of structurally distinct substrates without a loss of function is of critical importance to expand metabolic versatility (16). The bacterial biphenyl (BPH) catabolic pathway represents an example of a new emerging pathway for the degradation of several man-made persistent pollutants such as polychlorinated biphenyls (5, 11, 19). The biphenyl dioxygenase (BPDO) catalyzes the initial dioxygenation of BPH (Fig. 1A). BPDOs are potentially capable of metabolizing several chlorobiphenyls. They are composed of three components, which in *Burkholderia xenovorans* LB400 are designated as follows (20–22): the catalytic component, a Rieske-type oxygenase (RO) protein (BphAE) made up of three α -subunits (BphA) and three β -subunits (BphE), as well as the ferredoxin (BphF) and the ferredoxin reductase (BphG), which are required to transfer electrons from NADH to BphAE. BphAE catalyzes a 2,3 (*ortho-meta*)-dihydroxylation toward biphenyl, but the regiospecificity of BphAE differs for different substrates. The substrate range and regiospecificity are principally determined by residues located on the C-terminal portion of the dioxygenase α -subunit, some of which are in contact with and others of which are removed from the substrate (19, 23–25).

BphAE_{LB400} from *B. xenovorans* LB400, which metabolizes a wide range of PCBs, is one of the most effective dioxygenases of natural origin. The BphAE_{LB400} substrate range can be altered by mutations that modulate the plasticity of the catalytic pocket to create the space required to accommodate substrates exhibiting structurally different conformations. A route to change the substrate range involves alterations of the side chains of residues lining the catalytic pocket. Residues such as Ser283 of BphAE_{LB400} line the entranceway of the catalytic pocket and may play a role in substrate specificity (Fig. 1B). Dhindwal et al. (26) observed that Ser283 is part of a small segment that moves during substrate binding, and its displacement differs depending on the dioxygenase and the mutants that are analyzed. In most BPDOs, this position is occupied by a nonpolar residue (Met, Ile, or Leu), whereas in BphAE_{LB400} it is occupied by Ser, a polar amino acid (Fig. 1C). In a previous report, strains with KF707-type specificity degraded a relatively narrow range of PCB congeners and were generally able to oxidize only lower chlorinated congeners (27). The enzymes designated as having KF707-type specificity, which have Leu or Ile at position 283, also showed the same issue (27). In BphAE_{B356} from *Pandoraea pnomenusa* B356, which is another effective PCB-degrading BPDO that metabolizes a different range of PCB congeners than BphAE_{LB400} (28), this position is occupied by a Met. Consequently, this residue thus appears of interest for engineering. Additionally, the BphAE_{p4} and BphAE_{RR41} variants were derived from BphAE_{LB400} (29, 30). BphAE_{p4} was created by a double substi-

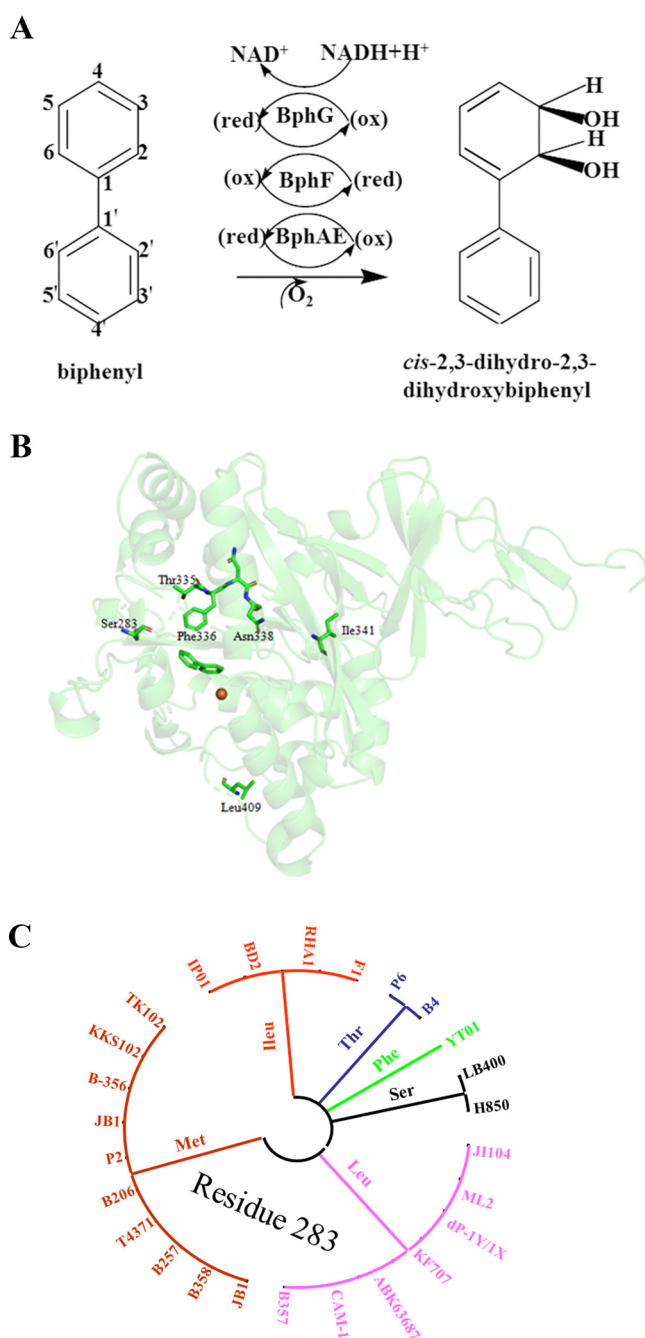


FIG 1 The biphenyl dioxygenase reaction, its structure, and the variability of residue 283. (A) BPDO reaction. BphG is the reductase, and BphF is the ferredoxin. red, reduction reaction; ox, oxidation reaction. (B) Positions of residues 283, 335, 336, 338, 341, and 409 in the crystal structure of the alpha subunit of BphAE_{LB400}. (C) Ser283 of LB400 BPDO is replaced by Thr, Ile, Met, or Leu in other BPDOs or other homologous dioxygenases. Details about the dioxygenases in panel C are shown in Table S1 in the supplemental material.

tution of BphAE_{LB400} Thr335 Phe336 to Ala335 Met336 (29). BphAE_{RR41} was obtained by replacing Asn338 Ile341 Leu409 of BphAE_{p4} with Gln338 Val341 Phe409 (30). Compared to BphAE_{LB400}, BphAE_{p4} metabolizes an expanded range of chlorobiphenyls, and it exhibits an enhanced ability to metabolize the coplanar compound dibenzofuran. BphAE_{RR41} also exhibits an ability to metabolize a broader range of PCB congeners than BphAE_{p4} and BphAE_{LB400} (31). Kumar et al. (32) identified that the Thr335Ala substitution contributes the most to the new properties of BphAE_{p4}. Residue Thr335 of BphAE_{LB400} imposes con-

straints through polar contacts to the segment spanning Val320, Gly321, and Gln322 lining the catalytic pocket (Fig. 1B). Mutating Thr335 to Ala reduces these constraints and thus increases the space available so that the bulkier chlorinated biphenyl can be accommodated in the catalytic pocket. The superior ability of BphAE_{RR41} to metabolize dibenzofuran over BphAE_{p4} is caused by the double substitutions Asn338Gln and Leu409Phe, both of which are essential to confer the new catalytic properties to BphAE_{RR41} (33). Both residues are far from the substrate, but together, they influence subunit assembly and the substrate-induced conformation of reaction-critical atoms (33).

In this context, we mutated Ser283 of BphAE_{LB400}, BphAE_{p4}, and BphAE_{RR41} to Met as in BphAE_{B356} to generate BphAE_{S283M}, BphAE_{p4-S283M}, and BphAE_{RR41-S283M}, respectively. We compared some of the catalytic properties of BphAE_{LB400}, BphAE_{p4}, BphAE_{RR41}, BphAE_{S283M}, BphAE_{p4-S283M}, and BphAE_{RR41-S283M} toward biphenyl and selected PCB congeners, and we also modeled the structures of BphAE_{S283M}, BphAE_{p4-S283M}, and BphAE_{RR41-S283M} and the docked substrates in order to investigate the structural features of BphAEs responsible for the differential catalytic properties of these enzymes.

RESULTS

Production of BphAE_{LB400} and its variants. Various recombinant BphAEs were produced and purified as His-tagged proteins as described in Materials and Methods. Each His-tagged BphAE protein was examined by SDS-PAGE; only two single bands were observed, corresponding to the α -subunit (BphA [M_r = 51,000]) and the β -subunit (BphE [M_r = 22,000]) (see Fig. S1 in the supplemental material).

Steady-state kinetics of BphAE_{LB400} and its variants toward BPH and PCB congeners. Based on biochemical data, the Ser283Met mutation in BphAE_{LB400} significantly enhanced the enzyme's PCB-degrading potential, the same mutation in BphAE_{p4} did not produce such a significant effect, and this mutation in BphAE_{RR41} hindered the PCB-degrading potential of the enzyme. However, the Ser283Met mutation altered the regiospecificity of BphAE_{RR41} based on biochemical data and structural analysis. Additionally, BphAE_{RR41} exhibited the ability to metabolize a broad range of PCB congeners compared to BphAE_{p4} and BphAE_{LB400} (31). Thus, BphAE_{LB400}, BphAE_{S283M}, BphAE_{RR41}, and BphAE_{RR41-S283M} were chosen for kinetic analyses with lower chlorinated congeners of PCB. Meanwhile, to date, little is known about the degradation of highly chlorinated biphenyls, especially the kinetics of highly chlorinated PCB degradation by enzymes (3). In the present work, BphAE_{S283M} metabolized highly chlorinated biphenyls significantly better than other variants. Consequently, BphAE_{LB400} and BphAE_{S283M} were chosen for kinetic analyses with highly chlorinated biphenyls. The steady-state kinetic parameters of BphAE_{LB400} and its variants toward PCBs were calculated from oxygen consumption using an oxygraph. The k_{cat}/K_m values for BphAE_{LB400} and its variants are given in Table 1 and Table S3. In order to read and understand the results, catalytic activities that were improved are shown in Table 1, and those that were unchanged or worse are shown in Table S3. The k_{cat}/K_m value for BphAE_{S283M} was four times higher than that for BphAE_{LB400} toward biphenyl (Table 1). The k_{cat}/K_m values for BphAE_{p4-S283M} and BphAE_{RR41-S283M} were also improved compared to BphAE_{LB400} toward biphenyl (Table 1). This result demonstrated the enhanced ability of BphAE_{S283M}, BphAE_{p4-S283M}, and BphAE_{RR41-S283M} to metabolize biphenyl compared with BphAE_{LB400}, BphAE_{p4}, and BphAE_{RR41}. The Ser283Met substitution lowered the k_{cat}/K_m for the reaction with 4-CB (Table S3). Additionally, compared to BphAE_{RR41}, BphAE_{RR41-S283M} showed a low k_{cat}/K_m value with 4-chlorobiphenyl (4-CB) (Table S3). On the other hand, the Ser283Met substitution did not affect the value of the specificity constant toward 2,2'-dichlorobiphenyl (2,2'-CB) for both BphAE_{LB400} and BphAE_{RR41} (Table S3). Compared with the three above-described congeners, BphAE_{LB400} and BphAE_{RR41} exhibited a low apparent specificity toward 2,5-dichlorobiphenyl (2,5-CB) and 2,6-dichlorobiphenyl (2,6-CB), and the Ser283Met substitution did not improve it. For some of these enzymes, the kinetic parameter values were even too low to be measured. In the case of 2,2',5,5'-

TABLE 1 Steady-state kinetic parameters of BPDO variants^a

Substrate and enzyme	Mean K_m (μM) \pm SD	Mean k_{cat} (s^{-1}) \pm SD	k_{cat}/K_m ($10^3 \text{ M}^{-1} \text{ s}^{-1}$)
BPH			
BphAE _{LB400}	35.0 \pm 4	1.1 \pm 0.1	32.2
BphAE _{S283M}	17.3 \pm 0.4	2.2 \pm 0.0	126.6
BphAE _{p4}	53.3 \pm 15	1.0 \pm 0.2	18.3
BphAE _{p4-S283M}	77.7 \pm 7	3.5 \pm 0.4	44.5
BphAE _{RR41}	59.6 \pm 10	0.7 \pm 0.2	12.6
BphAE _{RR41-S283M}	53.4 \pm 4	2.9 \pm 0.2	53.9
2,3',4,4'-CB			
BphAE _{LB400}	ND	ND	ND
BphAE _{S283M}	33.9 \pm 3	1.0 \pm 0.03	28.4
2,2',6,6'-CB			
BphAE _{LB400}	ND	ND	ND
BphAE _{S283M}	8.8 \pm 0.8	0.3 \pm 0.01	34.8
2,3',4,4',5-CB			
BphAE _{LB400}	ND	ND	ND
BphAE _{S283M}	33.0 \pm 12	0.6 \pm 0.09	17.5

^aThe kinetic parameters were determined from oxygen uptake measurements as described in Materials and Methods. ND, the kinetic parameters for some of the enzymes could not be determined with certain substrates because the activity was too low, or the enzyme did not follow Michaelis-Menten kinetics.

tetrachlorobiphenyl (2,2',5,5'-CB), the k_{cat}/K_m value was not affected by the Ser283Met mutation, as shown in Table S3. However, for 2,3',4,4'-tetrachlorobiphenyl (2,3',4,4'-CB) and 2,2',6,6'-tetrachlorobiphenyl (2,2',6,6'-CB), the k_{cat}/K_m values for BphAE_{S283M} are in the same range as those for BphAE_{LB400} toward biphenyl. Meanwhile, 2,3',4,4',5-pentachlorobiphenyl (2,3',4,4',5-CB) was a good substrate for BphAE_{S283M} since its kinetic parameters were higher than those for 2,5-CB and 2,6-CB. Under the same experimental conditions, BphAE_{LB400} was poorly active toward 2,3',4,4'-CB, 2,2',6,6'-CB, and 2,3',4,4',5-CB. Thus, the Ser283Met substitution improved the catalytic abilities of the three congeners. Finally, the steady-state kinetic parameters of BphAE_{LB400} and BphAE_{S283M} toward 2,2',4,4',5,5'-hexachlorobiphenyl (2,2',4,4',5,5'-CB) were too low to be determined accurately, so they are not reported here. Together, the Ser283Met substitution enhanced the catalytic activity of BphAEs toward biphenyl, 2,3',4,4'-CB, 2,2',6,6'-CB, and 2,3',4,4',5-CB. Nevertheless, the Ser283Met substitution hindered the catalytic activity of BphAEs toward 4-CB, but in the case of 2,2'-CB, 2,5-CB, 2,6-CB, and 2,2',5,5'-CB, no significant effects were observed.

Metabolism of 2,2'-CB, 2,5-CB, and 2,6-CB by BphAE_{LB400} variants. The regio-specificity of BPDO influences the products that are formed, which influences the catalytic degradation of the substrates by the subsequent enzymes of the pathway. 2,2'- and 2,6-dichlorobiphenyls belonging to the *ortho*-substituted PCB congeners are among the PCB congeners most resistant to microbial attack (29). In a previous report, the variants of BphAE_{LB400} that oxygenate 2,2'-dichlorobiphenyl at a higher rate than their parental enzyme were able to metabolize a broader range of PCB congeners than BphAE_{LB400} (18). In addition, as previously reported, unlike BphAE_{LB400}, BphAE_{B356} metabolizes 2,6-dichlorobiphenyl efficiently (34). On the other hand, unlike BphAE_{B356}, which oxygenates 2,5-dichlorobiphenyl into the *ortho-meta* position of the unsubstituted ring only, BphAE_{LB400} can oxygenate this substrate into the *meta-para* position (35). Thus, 2,2'-, 2,5-, and 2,6-dichlorobiphenyls were chosen for kinetic analyses, and the metabolites generated from these substrates by BphAE_{LB400} and its variants were identified. The metabolites were identified by gas chromatography-time of flight mass spectrometry (GC-TOF-MS) analysis as described in Materials and Methods. In the case of 2,2'-dichlorobiphenyl, two metabolites were produced by the BphAEs (Fig. 2). The mass spectrum of the first metabolite's *n*BuB (*n*-butylboronate) derivative was in agreement with a dihydro-dihydroxy-chlorobiphenyl described in previous works (22,

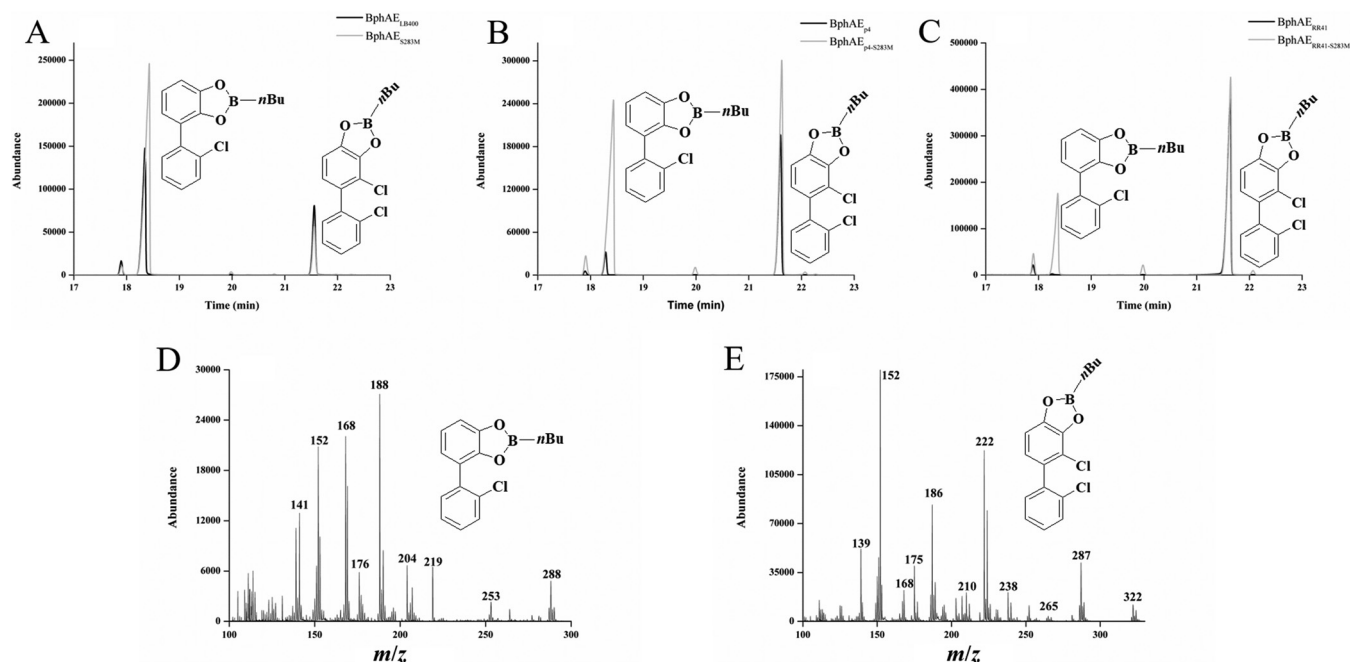


FIG 2 GC-MS spectra of butylboronate-derived metabolites produced from 2,2'-CB by reconstituted His-tagged BphAE_{LB400} and its variants. (A) Total ion chromatogram showing the peaks of metabolites produced from 2,2'-CB by reconstituted His-tagged BphAE_{LB400} and BphAE_{S283M}. (B) Total ion chromatogram showing the peaks of metabolites produced from 2,2'-CB by reconstituted His-tagged BphAE_{p4} and BphAE_{p4-S283M}. (C) Total ion chromatogram showing the peaks of metabolites produced from 2,2'-CB by reconstituted His-tagged BphAE_{RR41} and BphAE_{RR41-S283M}. (D) Mass spectrum of the metabolite exhibiting a retention time of 18.3 min. (E) Mass spectrum of the metabolite exhibiting a retention time of 21.5 min.

32). It was characterized by a fragmentation pattern exhibiting a molecular ion at m/z 288 and diagnostically important ions at m/z 253 ($M^+ - Cl$), m/z 204 ($M^+ - C_4H_9BO$), and m/z 188 ($M^+ - C_4H_9BO_2$) (Fig. 2D). The mass spectral features of the second metabolite are shown in Fig. 2E, with the characteristic molecular ion (m/z 322) and a fragmentation pattern exhibiting diagnostically important ions at m/z 287 ($M^+ - Cl$), m/z 265 ($M^+ - n$ -butyl), m/z 238 ($M^+ - C_4H_9BO$), and m/z 222 ($M^+ - C_4H_9BO_2$), corresponding to the 3,4-dihydro-3,4-dihydroxy-2,2'-dichlorobiphenyl previously described as the minor metabolite of BphAE_{LB400}. BphAE_{p4} and BphAE_{RR41} generated principally 3,4-dihydro-3,4-dihydroxy-2,2'-dichlorobiphenyl and small amounts of 2,3-dihydro-2,3-dihydroxy-2'-chlorobiphenyl (Fig. 2B and C). The major metabolite produced by BphAE_{LB400} and BphAE_{S283M} was identified as 2,3-dihydro-2,3-dihydroxy-2'-chlorobiphenyl (Table 2), but the proportion of the dehalogenated

TABLE 2 Metabolite patterns of variant BphAEs

Substrate and metabolite	RT (min) ^b	Metabolite ratio (SD) ^a					
		BphAE _{LB400}	BphAE _{S283M}	BphAE _{p4}	BphAE _{p4-S283M}	BphAE _{RR41}	BphAE _{RR41-S283M}
2,2'-CB							
2,3-Dihydro-2,3-dihydroxy-2'-chlorobiphenyl	18.3	68 (12.8)	84 (4)	22 (7.7)	43 (13.7)	1 (1)	34 (5.6)
3,4-Dihydro-3,4-dihydroxy-2,2'-dichlorobiphenyl	21.55	32 (12.8)	16 (4)	78 (7.7)	57 (13.7)	99 (1)	66 (5.6)
2,5-CB							
2',3'-Dihydro-2',3'-dihydroxy-2,5-dichlorobiphenyl	21.8	98.3 (0.2)	98 (1.7)	98 (0.3)	95 (0.2)	97 (0.5)	96 (0)
3,4-Dihydro-3,4-dihydroxy-2,5-dichlorobiphenyl	22.7	0.9 (0.2)	1.6 (1.7)	1 (0.3)	4 (0.2)	2 (0.5)	4 (0)
3',4'-Dihydro-3',4'-dihydroxy-2,5-dichlorobiphenyl	23.4	0.8 (0.2)	0.4 (1.7)	1 (0.3)	1 (0.2)	1 (0.5)	0 (0)
2,6-CB							
3',4'-Dihydro-3',4'-dihydroxy-2,6-dichlorobiphenyl	21.5	5 (0.9)	4 (1.8)	37 (1.8)	75 (1.5)	38 (17)	80 (0.7)
2',3'-Dihydro-2',3'-dihydroxy-2,6-dichlorobiphenyl	22.7	95 (0.9)	96 (1.8)	63 (1.8)	25 (1.5)	62 (17)	20 (0.7)

^aMetabolite ratio based on the areas of the peaks of metabolites detected by gas chromatography-time of flight mass spectrometer (GC-TOF-MS) analysis of butylboronate-derived metabolites produced by purified enzyme preparations. Standard deviations are indicated in parentheses.

^bRT is the retention time (in minutes) of each metabolite under the chromatographic conditions used.

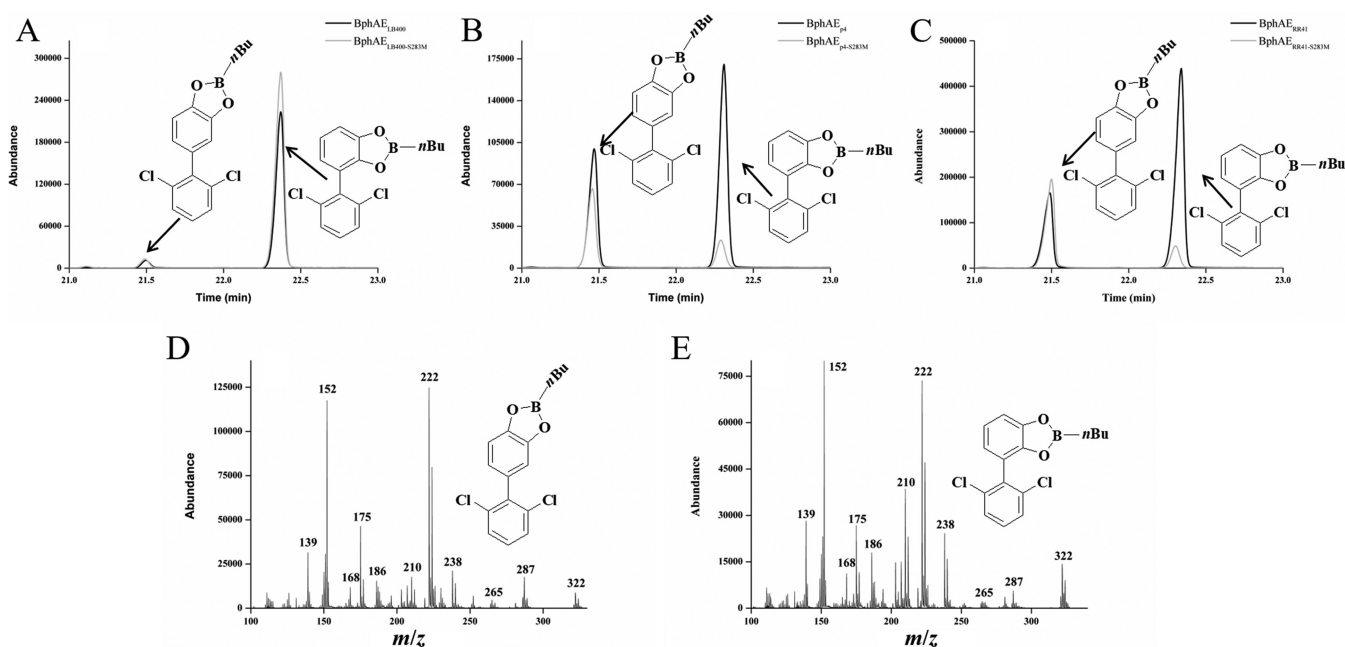


FIG 3 GC-MS spectra of butylboronate (nBu)-derived metabolites produced from 2,6-CB by reconstituted His-tagged BphAE_{LB400} and its variants. (A) Total ion chromatogram showing the peaks of metabolites produced from 2,6-CB by reconstituted His-tagged BphAE_{LB400} and BphAE_{LB400-S283M}. (B) Total ion chromatogram showing the peaks of metabolites produced from 2,6-CB by reconstituted His-tagged BphAE_{p4} and BphAE_{p4-S283M}. (C) Total ion chromatogram showing the peaks of metabolites produced from 2,6-CB by reconstituted His-tagged BphAE_{RR41} and BphAE_{RR41-S283M}. (D) Mass spectrum of the metabolite exhibiting a retention time of 21.5 min. (E) Mass spectrum of the metabolite exhibiting a retention time of 22.7 min.

metabolite was slightly increased in the Ser283Met variant. BphAE_{RR41} and BphAE_{p4} principally produced 3,4-dihydro-3,4-dihydroxy-2,2'-dichlorobiphenyl, but their respective BphAE_{RR41-S283M} and BphAE_{p4-S283M} derivatives produced significantly more 2,3-dihydro-2,3-dihydroxy-2'-chlorobiphenyl than their parents (Table 2). The fact that the ratio of 2,3-dihydro-2,3-dihydroxy-2'-chlorobiphenyl to 3,4-dihydro-3,4-dihydroxy-2,2'-dichlorobiphenyl is higher in all the Ser283Met variants than in their parental enzymes indicates that the regiospecificity toward 2,2'-dichlorobiphenyl is influenced by the Ser283Met substitution.

In the case of 2,6-dichlorobiphenyl, BphAEs produced two dihydro-dihydroxy-dichlorinated metabolites of 2,6-dichlorobiphenyl (Fig. 3). Both of them reflected a fragmentation pattern comprising ions at m/z 287 ($M^+ - Cl$), m/z 265 ($M^+ - n\text{-butyl}$), m/z 238 ($M^+ - C_4H_9BO$), and m/z 222 ($M^+ - C_4H_9BO_2$) that was consistent with data from a previous report, as shown in Fig. 3D and E (22). The substrate was majorly converted to 2',3'-dihydro-2',3'-dihydroxy-2,6-dichlorobiphenyl by BphAE_{LB400} and BphAE_{S283M} (Fig. 3A). BphAE_{p4} and BphAE_{RR41} yielded 2',3'-dihydroxy-2,6-dichlorobiphenyl as the major metabolite, whereas BphAE_{p4-S283M} and BphAE_{RR41-S283M} produced principally 3',4'-dihydro-3',4'-dihydroxy-2,6-dichlorobiphenyl (Fig. 3B and C). Notably, the ratio of 2',3'-dihydro-2',3'-dihydroxy-2,6-dichlorobiphenyl to 3',4'-dihydro-3',4'-dihydroxy-2,6-dichlorobiphenyl is lower in the BphAE_{RR41-S283M} and BphAE_{p4-S283M} variants than in their respective parental enzymes (Table 3). Consequently, for 2,6-CB, there is a marked effect of p4 and RR41 where the metabolite ratio is inverted. This represents the preferential production of 3',4'-dihydro-3',4'-dihydroxy-2,6-dichlorobiphenyl by Ser283Met variants compared to their parental enzymes. Altogether, these results indicate that the Ser283Met substitution alters the dioxygenation site of the substrate and thereby produces comparatively different metabolites.

Whole-cell assays to evaluate the PCB-degrading potential. Steady-state kinetic parameters for highly chlorinated biphenyls were not determined in this work due to the low solubility of highly chlorinated PCB congeners, the low activities of the

TABLE 3 Percent degradation of PCB congeners by BphAE variants

Congener	% degradation by mutant ^a					
	BphAE _{LB400}	BphAE _{S283M}	BphAE _{p4}	BphAE _{p4-S283M}	BphAE _{RR41}	BphAE _{RR41-S283M}
2,3',4-CB	19.3	62.5	53.1	34.3	57.8	33.6
2,4,4'-CB	18.3	22.6	37.9	51.1	43.6	32.2
2,2',5,5'-CB	52.9	68.6	68.6	56.3	64.5	32.4
2,2',6,6'-CB	10.6	99.2	29.1	61.2	24.0	41.5
2,3',4,4'-CB	13.3	97.1	N	69.3	39.5	27.8
3,3',4,4'-CB	19.6	61.2	33.7	45.0	39.5	27.8
2,2',3,4,5'-CB	19.2	65.3	31.7	44.0	40.7	27.5
2,3',4,4',5-CB	16.7	65.1	27.7	45.7	38.1	23.5
2,2',3,4,5,5'-CB	11.4	69.2	18.0	51.4	39.2	22.6
2,2',4,4',5,5'-CB	14.6	71.7	22.4	50.6	36.1	20.0

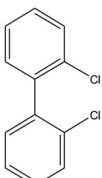
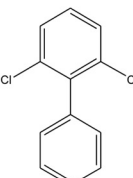
^aShown is the percent depletion of each PCB congener of a mix of 10 congeners added to a culture of *E. coli* DH11(pQE51[LB400-*bphFG*]/pDB31[LB400-*bphFG*]) expressing the indicated BphAEs. These resting cell assay mixtures were incubated for 18 h before the remaining PCBs were measured. The values are averages from three separate experiments done in triplicate. The variance was <10% of the measured values in all cases. N, no degradation, or the level of depletion was not statistically significant compared to the negative control. Statistical significance was determined according to the *t* test ($P \leq 0.05$). 4-CB is not shown because the mutant enzymes were not active with this substrate.

isozymes, and the poor coupling of the transformation of the highly chlorinated biphenyls to O₂ consumption (36). However, several meaningful studies using whole-cell degradation assays provide valuable insights into the capacity of the enzyme (18, 19, 25, 31, 36). Thus, we assessed the capacity of recombinant *Escherichia coli* DH11S cells with BpAE_{LB400} and its variants to degrade PCB congeners. The degradation data are summarized in Table 3. 4-CB is not shown because the mutant enzymes were not active with this substrate. In a previous report, BphAE_{p4} exhibited a higher potency toward 2,3',4-trichlorobiphenyl (2,3',4-CB) and 2,4,4'-trichlorobiphenyl (2,4,4'-CB) than BphAE_{LB400} (28). In the present work, 2,3',4-CB was depleted significantly better by BphAE_{S283M} than by BphAE_{LB400}, but BphAE_{S283M} did not perform better than BphAE_{p4} toward 2,4,4'-CB. As shown in a previous report (37), BphAE_{LB400} and BphAE_{p4} metabolized the *ortho-meta* congener 2,2',5,5'-CB, and their respective Ser283Met variants metabolized this substrate similarly. Notably, 2,2',6,6'-CB, an *ortho*-substituted PCB congener, which is one of the PCB congeners most resistant to microbiological degradation, was depleted significantly in our assay by BphAE_{S283M} compared to the other variants. Consistent with previous reports (28, 31), the *mono-ortho* coplanar congener 2,3',4,4'-CB is very poorly oxygenated by BphAE_{LB400}, whereas BphAE_{RR41} degrades it better. Notably, BphAE_{S283M} and BphAE_{p4-S283M} metabolized 2,3',4,4'-CB significantly better than BphAE_{LB400} and its variants. Barriault et al. (28) previously reported that 2,2',3,4,5'-pentachlorobiphenyl (2,2',3,4,5'-CB) was poorly degraded by BphAE_{LB400} and BphAE_{p4}. Its degradation was improved for BphAE_{RR41} compared to BphAE_{LB400} and BphAE_{p4} (31). However, it is noteworthy that BphAE_{S283M} metabolized 2,2',3,4,5'-CB significantly better than BphAE_{RR41}. Additionally, based on previous reports that highly chlorinated biphenyls such as 2,3',4,4',5-CB, 2,2',3,4,5,5'-hexachlorobiphenyl (2,2',3,4,5,5'-CB), and 2,2',4,4',5,5'-CB were metabolized poorly by biphenyl dioxygenase (18, 19, 29, 31, 36), we assessed the capacity of BpAE_{LB400} and its variants to degrade these three highly chlorinated biphenyls. The results demonstrated that these three congeners were metabolized significantly by BphAE_{S283M}.

It is noteworthy that 11 PCB congeners were depleted significantly by BphAE_{S283M}. With the exception of 2,4,4'-CB, BphAE_{S283M} metabolized a broader range of the 11 congeners than cells expressing BphAE_{p4} (Table 3). BphAE_{S283M} exhibits an enhanced ability to metabolize the 10 congeners compared to BphAE_{p4} and BpAE_{RR41}. This indicates a meaningful contribution of Met283 of BphAE_{S283M} to the selectivity of some PCB substrates. Similarly, BphAE_{p4-S283M} performed better than BphAE_{p4} in the degradation of most of the tested congeners except 2,3',4-CB and 2,2',5,5'-CB. However, in contrast, the Ser283Met mutation negatively affected the ability of BphAE_{RR41} to oxygenate these congeners.

Structural analysis of docked 2,2'-CB and 2,6-CB at active sites of BphAE_{LB400} and its variants. In order to provide insight into structural features of BphAE_{LB400} and

TABLE 4 Probable sites for dioxygenation, distances from these carbons to Fe^{2+} , and binding energies for docking of 2,2'-dichlorobiphenyl and 2,6-dichlorobiphenyl at the active sites of BphAE_{LB400}, BphAE_{S283M}, BphAE_{p4}, BphAE_{p4-S283M}, BphAE_{RR41}, and BphAE_{RR41-S283M}

PCB and structure	BPDO variant	Carbon positions for dioxygenation	Dioxygenation ^a	Distance (Å) from Fe^{2+}			Binding Energy
				C-2	C-3	C-4	
2,2'-Dichlorobiphenyl 	LB400	2, 3	<i>o, m</i>	4.0	4.3	5.0	-7.33
	S283M	2, 3	<i>o, m</i>	4.0	4.3	5.0	-6.64
	p4	2, 3 or 3, 4	<i>o, m</i> or <i>m, p</i>	4.8	4.3	4.8	-7.05
	p4-S283M	2, 3 or 3, 4	<i>o, m</i> or <i>m, p</i>	4.6	4.1	4.6	-7.98
	RR41-S283M	3, 4	<i>m, p</i>	4.6	4.0	4.5	-7.44
2,6-Dichlorobiphenyl 	LB400	2' 3'	<i>o, m</i>	3.7	4.6	5.9	-7.26
	S283M	2' 3'	<i>o, m</i>	4.3	5.0	5.8	-5.74
	p4 ^b	2' 3' or 3' 4'	<i>o, m</i> or <i>m, p</i>	4.9	4.6	4.9	
	p4-S283M	3' 4'	<i>m, p</i>	5.0	4.5	4.6	-6.95
	RR41	2' 3'	<i>o, m</i>	4.7	4.5	5.0	-6.98
	RR41-S283M	3' 4'	<i>m, p</i>	5.1	4.6	4.6	-7.14

^a*o, m*, ortho-meta dioxygenation; *m, p*, meta-para dioxygenation.

^bBphAE_{p4} with the 2,6-dichlorobiphenyl-bound form (RCSB PDB accession number 2XSH) was prepared as previously described (66).

its variants that elucidate why these enzymes catalyze 2,2'-CB and 2,6-CB oxidation differently, we docked 2,2'-CB and 2,6-CB at their active sites. The probable sites for dioxygenation, distances from these carbons to Fe^{2+} , and binding energies for the docking of 2,2'-dichlorobiphenyl and 2,6-dichlorobiphenyl at the active sites of BphAE_{LB400}, BphAE_{S283M}, BphAE_{p4}, BphAE_{p4-S283M}, BphAE_{RR41}, and BphAE_{RR41-S283M} are summarized in Table 4. For BphAE_{S283M}, 2,2'-CB docked similarly in the same position and orientation as in BphAE_{LB400}. The C-2 chlorine atoms and C-3 of the reactive ring of 2,2'-CB in BphAE_{S283M} closely aligned with C-2 chlorine atoms and C-3 of the reactive ring of 2,2'-CB in BphAE_{LB400} (Fig. 4A). This result is consistent with the biochemical data. In this orientation, C-2 and C-3 are 4.0 Å and 4.3 Å away from the Fe^{2+} ion, respectively. This shows that the primary metabolite produced from 2,2'-CB when

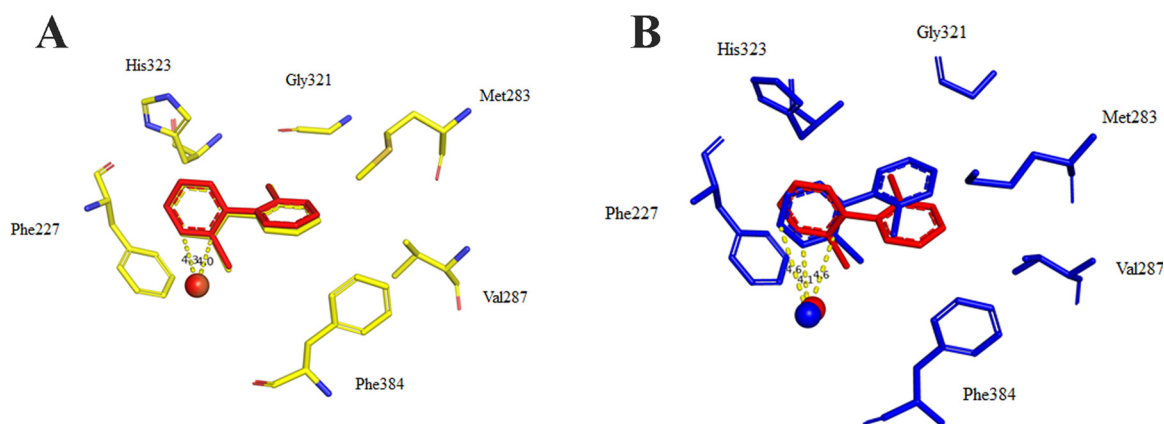


FIG 4 (A) Superposition of catalytic center residues of the 2,2'-CB-docked forms of BphAE_{S283M} (yellow) and BphAE_{LB400} (red). (B) Superposition of catalytic center residues of the 2,2'-CB-docked form of BphAE_{p4-S283M} (blue) and BphAE_{LB400} (red).

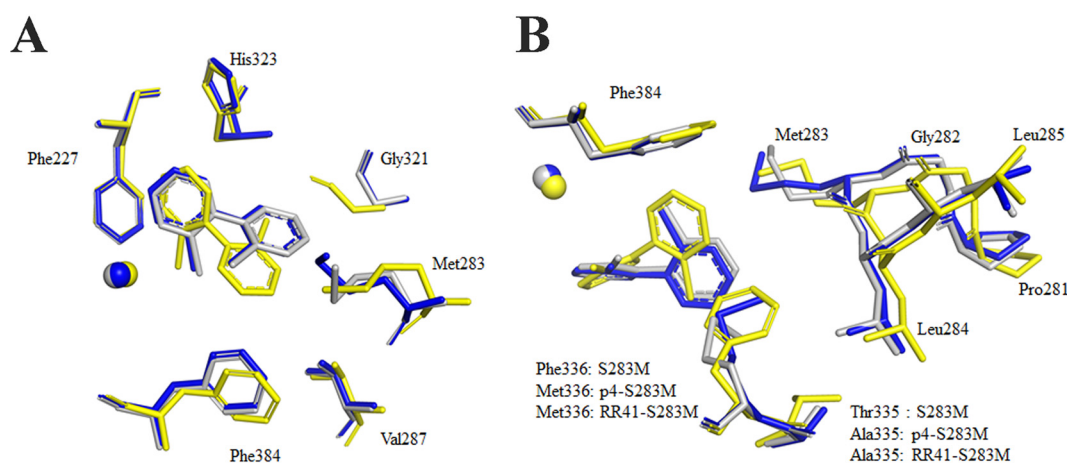


FIG 5 Superpositions of catalytic center residues of the 2,2'-CB-docked forms of BphAE_{S283M} (yellow), BphAE_{p4-S283M} (blue), and BphAE_{RR41-S283M} (gray).

BphAE_{S283M} catalyzes the reaction would be 2,3-dihydro-2,3-dihydroxy-2'-chlorobiphenyl. However, for BphAE_{p4-S283M}, the docking of 2,2'-CB produced an orientation different from that of BphAE_{LB400}. The proximal ring is approximately aligned with the reactive ring of 2,2'-CB in the complex form of BphAE_{LB400}, but the distal ring is shifted toward Gly321 in BphAE_{p4-S283M} (Fig. 4B). The distances from the Fe²⁺ ion to C-2, C-3, and C-4 are 4.6 Å, 4.1 Å, and 4.6 Å, respectively. Hence, hydroxylation would occur on carbons 2 and 3 or 3 and 4 to produce 2,3-dihydro-2,3-dihydroxy-2'-chlorobiphenyl and 3,4-dihydro-3,4-dihydroxy-2,2'-dichlorobiphenyl. This result is also in agreement with biochemical data. For BphAE_{RR41-S283M}, the docking of 2,2'-CB produced an orientation consistent with the same regiospecificity as those for BphAE_{p4-S283M} (Fig. 5A).

Homology modeling suggested that several residues near the distal ring of the substrate, such as Met283, Gly321, and Phe384, move in the BphAE_{S283M} structure (Fig. 5A). These residues modulate the conformation of the distal ring of 2,2'-CB toward Phe384. The C-2 and C-3 of the reactive ring are closer to Fe²⁺ in BphAE_{S283M} than in BphAE_{p4-S283M} and BphAE_{RR41-S283M}. These results show that the regiospecificity of the enzyme is significantly dependent on residue Ser283. This modeling result suggests that the segment from positions 281 to 285 and Phe384 of BphAE_{S283M} are farther from the Fe²⁺ ion than in BphAE_{p4-S283M} and BphAE_{RR41-S283M} (Fig. 5B). This variation results in the cavity volume of BphAE_{S283M} being larger than those of BphAE_{p4-S283M} and BphAE_{RR41-S283M}. These results may explain why the k_{cat}/K_m value of BphAE_{S283M} toward 2,2'-CB is slightly higher than that of BphAE_{RR41-S283M}.

In order to further explore how the Ser283Met substitution affects 2,2'-CB binding, we also examined structural features of the segment from positions 281 to 284 in the different enzymes. As shown in Fig. S2A, although Ser is replaced by Met, the conformation of 2,2'-CB in the complex form of BphAE_{S283M} is similar to that of BphAE_{LB400}. When Ser is replaced by Met in BphAE_{p4-S283M}, the 2,2'-CB ligand moves farther from Met283 (Fig. S2B).

2,6-CB was also docked into BphAE_{LB400} and its variants. Compared with the orientation of 2,6-CB in the previously studied variant BphAE_{p4}, the conformation of the docked substrate in BphAE_{S283M} is opposite the ring of 2,6-CB in BphAE_{p4} (Fig. 6A). The distances from the catalytic iron to C-2' and C-3' are 4.3 Å and 5.0 Å, respectively. According to the biochemical data, when BphAE_{S283M} catalyzed the reaction, the main primary metabolite produced from 2,6-CB was 2',3'-dihydro-2',3'-dihydroxy-2,6-dichlorobiphenyl. Residues Gly321 and Met283 are responsible for the reversal of rings of 2,6-CB in the opposite orientation (Fig. 6A). For BphAE_{p4-S283M}, when the docked substrate was superposed to 2,6-CB-bound BphAE_{p4}, the reactive ring of 2,6-CB in BphAE_{p4-S283M} was found in an orientation similar to that of the reactive ring in

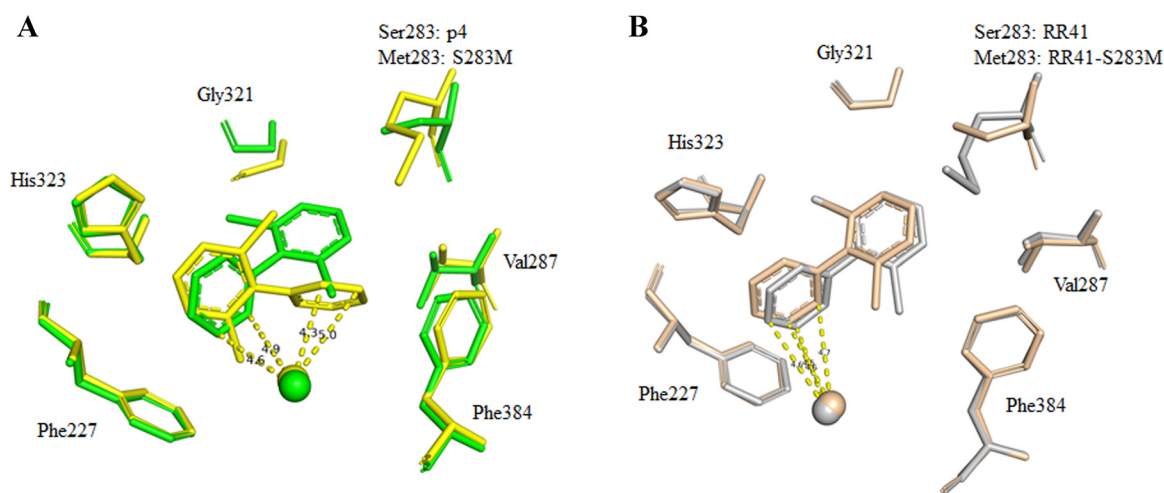


FIG 6 (A) Superposition of catalytic center residues of the 2,6-CB-docked forms of BphAE_{p4} (green) and BphAE_{p4-S283M} (yellow). (B) Superposition of catalytic center residues of the 2,6-CB-docked forms of BphAE_{RR41} (wheat) and BphAE_{RR41-S283M} (gray).

BphAE_{p4}. In the case of 2,6-CB-docked BphAE_{p4-S283M}, C-3' and C-4' are 4.5 Å and 4.6 Å away from the Fe²⁺ ion. This conformation is consistent with the biochemical data. The distances from C-3' and C-4' to iron in BphAE_{p4} are 4.6 Å and 4.9 Å. The replacement of Ser283 by Met in BphAE_{p4-S283M} did not create orientation changes compared with BphAE_{p4} (Fig. S3A). For BphAE_{RR41-S283M}, the docking of 2,6-CB produced a conformation consistent with the same regiospecificity as that for BphAE_{p4} (Fig. S3B). However, the conformation of docked 2,6-CB in BphAE_{RR41-S283M} is different from that in BphAE_{RR41} (Fig. 6B). In the case of 2,6-CB-docked BphAE_{RR41-S283M}, C-3' and C-4' are closer to the Fe²⁺ ion (Table 4), but C-2' and C-3' are closer to the Fe²⁺ ion in BphAE_{RR41}. This change suggests that the Ser283Met mutation altered the regiospecificity of BphAE_{RR41}. Overall, the results suggest that the Ser283Met mutation causes changes in the orientation of the substrate and thereby produces different metabolites.

DISCUSSION

Polychlorinated biphenyls are commonly metabolized by the biphenyl degradation pathway of bacteria, and the substrate range of BPDO, which initiates degradation, will determine the range of congeners that the pathway metabolizes (38). BPDOs are potentially capable of metabolizing many BPH analogs and bicyclic- or tricyclic-fused heterocyclic aromatics such as dibenzofuran and flavonoids (17, 39, 40). In previous studies, three mechanisms through which BphAEs expand their substrate range have been identified. Using a semirational directed-evolution approach, BphAE_{p4} and BphAE_{RR41} variants were obtained, which exhibited broader substrate ranges than wild-type BphAE_{LB400} (29, 30). Variants BphAE_{S100}, BphAE_{S149}, and BphAE_{S151} that were obtained by shuffling soil DNA with LB400 *bphA* exhibited effective catalytic properties for di-*ortho*-substituted chlorobiphenyls (41).

However, engineering or evolving BPDOs that catalyze the oxidation of a wider range of PCBs is a formidable task. Many residues that are in contact with or removed from the substrate may alter catalytic properties. The mechanisms by which these residues act vary depending on the analog used as the substrate. Numerous enzyme-engineering reports on benzene, chlorobenzene, biphenyl, and naphthalene dioxygenases identified several amino acid residues of these Rieske-type oxygenases that can modulate substrate specificity and regiospecificity (15, 16, 42–46). The segment from positions 280 to 283 in BphAEs is located at the entrance of the catalytic pocket, and it shows conformational variations. Compared to BphAE_{LB400}, Ser283 of BphAE_{p4} shows a considerable shift after substrate binding (47). Ser283 also influences the activity of this enzyme toward di-*ortho*-substituted chlorobiphenyls (41), and Pham et al. reported that residue 283 was very close to ring A of flavone in flavone-docked BphAE_{p4} (18).

Based on the *Pseudomonas fluorescens* IP01 cumene dioxygenase crystal structure, the corresponding residue, L284, is part of a loop involved in the formation of the active site of this oxygenase (48). In most BPDOs, this position is occupied by a neutral residue (Met, Ile, or Leu), whereas in LB400, it is occupied by Ser, a charged amino acid. In this work, we further investigated the role of this residue in substrate specificity and regiospecificity. The BphAE_{S283M}, BphAE_{p4-S283M}, and BphAE_{RR41-S283M} variants were created from the parent enzymes BphAE_{LB400}, BphAE_{p4}, and BphAE_{RR41}, respectively, by the replacement of Ser283 with Met. We focused on the catalytic activity and degradation potential of BphAE variants toward *ortho*-substituted and highly chlorinated PCB congeners.

In previous reports, the k_{cat}/K_m value for BphAE_{LB400} toward biphenyl was found to be 10-fold higher than that for BphAE_{B356} (36). Our data show that the k_{cat}/K_m value toward this substrate was four times higher for BphAE_{S283M} than for BphAE_{LB400}. The k_{cat}/K_m value toward biphenyl for BphAE_{p4} was close to that for BphAE_{LB400} (33), and the kinetic parameters of BphAE_{LB400} toward biphenyl were higher than those of its variants BphAE_{II9} and BphAE_{II10} (18). To the best of our knowledge, the kinetics of the reaction of most previously described engineered BphAEs toward biphenyl are lower than those of their parental enzymes (18, 33, 49, 50). However, in this work, the k_{cat}/K_m values of the BphAE_{S283M}, BphAE_{p4-S283M}, and BphAE_{RR41-S283M} mutants toward biphenyl were higher than those of their respective parents.

Additionally, to date, the degradation of lower chlorinated congeners of PCB (chloride, ≤ 3) has been investigated extensively, but little is known about the degradation of highly chlorinated biphenyls, especially the kinetics of highly chlorinated PCB degradation by enzymes (3, 51–53). In this study, we determined the steady-state kinetics of BphAEs toward 2,3',4,4'-CB, 2,2',6,6'-CB, and 2,3',4,4',5-CB, which were found to be metabolized significantly better by the Ser283Met mutants than by their parent enzymes. Thus, for BphAEs displaying structural feature similar to those of BphAE_{LB400}, the Ser283Met mutation of BphAE_{LB400} variants may be a strategy to further enhance their catalytic activity toward biphenyl and highly chlorinated biphenyls.

Our results show that for 2,2'-CB, the ratio of 2,3-dihydro-2,3-dihydroxy-2'-chlorobiphenyl to 3,4-dihydro-3,4-dihydroxy-2,2'-dichlorobiphenyl is increased in all the Ser283Met variants compared to their parents. Although BphAE_{KF707} (the corresponding residue is a Leu), from *Pseudomonas alcaligenes* KF707, exhibits 95% identity with BphAE_{LB400}, it catalyzes a 5,6-dioxygenation of 2,2'-CB (54). Similarly, the previously described BphAE_{LB400} variants BphAE_{S100} (Leu283) and BphAE_{S151} (Met283) were also found to catalyze a 5,6-dioxygenation of 2,2'-CB (41). Those observations and ours may suggest that the residue located at position 283 plays a role in orienting the biphenyl ring toward the catalytic iron. In addition, the larger proportion of 2,3-dihydro-2,3-dihydroxy-2'-chlorobiphenyl that is produced from 2,2'-CB by the Ser283Met variants than by their respective parents suggests that the mutation allows a substrate orientation that favors catalytic oxygenolytic dehalogenation of this substrate. This is especially true for BphAE_{p4} but is also true for BphAE_{RR41}, which was previously reported to metabolize a broader range of PCB congeners than BphAE_{p4} and BphAE_{LB400} (30, 31). Structural analyses of 2,2'-CB-docked BphAE_{p4} and BphAE_{p4-S283M} show that the distance from catalytic Fe²⁺ to C-2 and C-4 is altered in the BphAE_{p4} variant carrying the Ser283Met substitution, which may explain why the Ser283Met mutation enhances the ability of the enzyme to catalyze 2,3-dioxygenation of 2,2'-CB.

In the case of 2,6-CB, based on biochemical data and structural analyses, we found that the Ser283Met mutation appears to favor a conformation to allow a 3,4-oxygenation of the unsubstituted ring. The BphAE_{S283M} variant produced the same metabolite ratio as BphAE_{LB400}. However, the Ser283Met mutation produced a significant effect on BphAE_{p4-S283M} and BphAE_{RR41-S283M}. In this case, the metabolite ratio was inversed compared to BphAE_{p4} and BphAE_{RR41}, where larger amounts of 3,4-dihydroxylated metabolites were produced in the variant enzymes. It is noteworthy that BphAE_{B356} (Met283) was reported to oxygenate carbons 3 and 4 of 2,6-CB (36).

Since the catalytic pocket of all these enzymes differed by a few amino acid residues, this observation further supports the hypothesis that residue 283 plays a role in the orientation of the substrate, but its influence varies greatly depending on the other protein residues with which it interacts during the substrate binding process.

We observed that the segment from positions 281 to 284 was displaced when 2,6-CB was docked in different enzymes. This result is consistent with a previous report that a short helix, including the segment from positions 282 to 288, needs to shift when 3,4-dihydroxylation occurred for BphAE_{B356} binding with 2,6-CB (36). Our structural analysis and the previous study demonstrated that the residue at position 283 is the only one on this helix that is in contact with the 2,6-dichlorobiphenyl. The docked data show that in the case of BphAE_{p4-S283M} and BphAE_{RR41-S283M} binding with 2,6-CB, the distal ring of 2,6-dichlorobiphenyl moved to *meta-para*-dioxygenation compared to their parent enzymes because of the larger size of Met. Furthermore, Dhindwal et al. found that Ser283 makes polar contact with Val320 in BphAE_{II9}. Ser283 also interacts with the chain of residues Ala286 and Val287 (26). Our analysis based on a homology model of BphAE_{p4-S283M} indicated that Met283 is far from Val320, which means that the constraint is released. However, the crystal structure of BphAE_{p4-S283M} will be required to explain this phenomenon more precisely.

Our structural analysis also identified Phe384 as another key residue lining the catalytic cavity that may influence substrate specificity and regiospecificity, where its interactions with other protein residues may influence the enzyme cavity volume. Our results corroborate those of Suenaga et al., who suggested that Phe383 of BphAE_{KF707} and the corresponding residue of BphAE_{LB400}, Phe384, may change either the range of substrates or the regiospecificity toward *ortho*-chlorinated biphenyls (55).

Furthermore, we assessed the substrate ranges of BphAE_{LB400} and its variants using a recombinant *E. coli* cell assay described previously (29). In previous reports (20, 31, 37), it was shown that all PCBs of a mix of 11 congeners similar to the one that we have used were metabolized at a low rate by BphAE_{LB400}. Compared to BphAE_{LB400}, BphAE_{p4} metabolized an expanded range of chlorobiphenyls, and it exhibited an enhanced ability to metabolize the coplanar compound dibenzofuran (27). BphAE_{RR41} exhibited the ability to metabolize a broader range of PCB congeners than BphAE_{p4} and BphAE_{LB400} (31). Our data show that the Ser283Met substitution extends the substrate ranges of BphAE_{LB400} and BphAE_{p4}. Thus, both BphAE_{S283M} and BphAE_{p4-S283M} exhibited a superior ability to metabolize the PCB mix over their respective parents. Numerous effective bacteria were isolated to degrade PCBs, such as *Pseudomonas*, *Polaromonas*, *Variovorax*, *Shigella*, *Janthinobacterium*, *Castellaniella*, and *Subtercola* (56–59). However, very few bacteria were reported to metabolize the most highly chlorinated PCBs. Notably, BphAE_{S283M} and BphAE_{p4-S283M} were able to degrade 10 congeners of the mix of 11 congeners described in Table S2 in the supplemental material, ranging from tri- to hexachlorinated biphenyls (Table 3). Thus, these variants may have the potential to remediate PCB pollution. However, given the complexity of the oxygenation of PCBs, it is rather difficult to understand clear-cut mechanisms to elucidate what determines the substrate range and how the enzymes evolve to expand their substrate range.

Nevertheless, although the Ser283Met mutation in BphAE_{LB400} significantly enhanced the enzyme's PCB-degrading potential, the same mutation in BphAE_{p4} did not produce such a significant effect, and in BphAE_{RR41}, this mutation hindered the PCB-degrading potential of the enzyme. BphAE_{p4} and BphAE_{RR41} differ from BphAE_{LB400} by only 2 and 5 amino acid residues, respectively, where both BphAE_{p4} and BphAE_{RR41} carry the same T335A F336M mutations. In previous reports, the Thr335Ala substitution in BphAE_{LB400} variants was found to broaden its substrate range, and the Phe336Met substitution affected the orientation of the substrate inside the catalytic pocket (32), whereas the Asn338Gln substitution in BphAE_{RR41} was shown to affect subunit assembly and stability by interacting indirectly with residue 409, which is far from it (31). The BPDO reaction is complex, where the RO component, which is itself composed of two subunits, needs to interact with two substrates (biphenyl and O₂) and electron transfer is required, which involves

TABLE 5 Sequence pattern of BphAE_{LB400} variants

Protein designation	Residue at position ^a :					
	283	335	336	338	341	409
BphAE _{LB400}	S	T	F	N	I	L
BphAE _{S283M}	M	T	F	N	I	L
BphAE _{p4}	S	A	M	N	I	L
BphAE _{p4-S283M}	M	A	M	N	I	L
BphAE _{RR41}	S	A	M	Q	V	F
BphAE _{RR41-S283M}	M	A	M	Q	V	F

^aAll other residues for these variants are identical to those for BphAE_{LB400}.

interactions between amino acids of the two RO subunits and between the RO and the ferredoxin. Previous studies (32, 33) have shown that many amino acid residues inside the active site or surrounding it interact with each other and with residues far away during substrate binding and catalytic reactions. Therefore, together, these data show that the changes required by this enzyme to modify the catalytic activity and substrate range are difficult to rationalize.

In conclusion, this study suggests that the Ser283Met substitution in BphAE_{LB400} variants influences the oxygenase catalytic reaction depending on the substrate and on the other protein residues with which it interacts. In some cases, this substitution may enhance the catalytic activity toward biphenyl, and it may alter the enzyme regiospecificity toward PCB congeners depending on their chlorine substitution pattern. Most notably, this residue may enhance the activity toward some of the more highly chlorinated biphenyls (3-6-chlorines), which are generally very poorly oxidized by most dioxygenases. The present work showed a dramatic effect of mutation Ser283Met on substrate specificity/regiospecificity in BPDO. This will certainly be a meaningful element for understanding the effect of the residue corresponding to position 283 in other Rieske oxygenase enzymes.

MATERIALS AND METHODS

Bacterial strains, plasmids, and chemicals. Wild-type strain *B. xenovorans* LB400 was described previously (60). *Escherichia coli* C41(DE3) (61) (Stratagene, La Jolla, CA) was used in this study. Plasmids pET14b[LB400-bphAE], pET14b[p4-bphAE], pET14b[RR41-bphAE], pET14b[LB400-bphF], pET14b[LB400-bphG], and pDB31[LB400-bphFG] were described previously (32, 33, 62). Chemical standards were purchased from Sigma-Aldrich. Biphenyl and PCB congeners were obtained from Accustandard (purity, >99%).

Preparation of Ser283Met mutants of each BphAE. A previously described two-step site-directed mutagenesis protocol (41) was utilized to create the three mutants with the single substitution Ser283Met in BphAE_{LB400}, BphAE_{p4}, and BphAE_{RR41} (Table 5). For each mutant, four primers were used to amplify two fragments that were assembled exactly as described previously by Vézina et al. (41). The right-end fragment was amplified using the forward primer 5'-GAGCCGGGCACGCTCTGGCG-3' with the reverse primer 5'-GGGGTACCCCTAGAAGAACATGCT-3', and the left-end side was amplified using the reverse primer 5'-GGGGTACCCCTAGAAGAACATGCT-3' with the forward primer 5'-CGGGATCCGATGAGTTCAGCAATCA-3'. BphAEs were expressed in *E. coli* C41(DE3) as His-tagged proteins and purified by affinity chromatography as described in a previous report (33). The level of expression of purified enzymes was assessed by SDS-PAGE (63).

Assays to determine the kinetic parameters of BphAE_{LB400}, BphAE_{p4}, BphAE_{RR41}, BphAE_{S283M}, BphAE_{p4-S283M}, and BphAE_{RR41-S283M} toward biphenyl and PCB congeners. Reconstituted His-tagged BPDO preparations were used to monitor enzyme activity and metabolite production. Variants were cloned in pET14b, expressed in *E. coli* C41(DE3), and purified by affinity chromatography as His-tagged enzymes as described previously by Mohammadi and Sylvestre (30). The concentration of each purified component was determined by spectrophotometry (20–22). The enzyme assays were performed at 37°C, according to a protocol described previously, in 1 ml in 50 mM morpholineethanesulfonic acid (MES) buffer containing 2.4 nmol of BphF, 1.2 nmol of BphG, 2.4 nmol of BphAE, and 400 nmol of NADH (22). PCB congeners included 4-chlorobiphenyl, 2,2'-dichlorobiphenyl (2,2'-CB), 2,5-dichlorobiphenyl (2,5-CB), 2,6-dichlorobiphenyl (2,6-CB), 2,2',5,5'-tetrachlorobiphenyl (2,2',5,5'-CB), 2,3',4,4'-tetrachlorobiphenyl (2,3',4,4'-CB), 2,2',6,6'-tetrachlorobiphenyl (2,2',6,6'-CB), 2,3',4,4',5-pentachlorobiphenyl (2,3',4,4',5-CB), and 2,2',4,4',5,5'-hexachlorobiphenyl (2,2',4,4',5,5'-CB). The steady-state kinetic parameters of all BphAEs were monitored by recording oxygen uptake for concentrations of selected PCBs between 5 and 60 μM (64). Kinetic parameters were obtained from the analysis of at least two independently purified preparations tested in triplicate.

Identification of the metabolites produced from 2,2'-CB, 2,5-CB, and 2,6-CB by BphAE_{LB400} and its variants. Reconstituted His-tagged BPDO preparations were utilized in these experiments. The

enzyme assays were performed as described above, at 37°C, in 50 mM MES buffer, and in a volume of 1 ml containing 2.4 nmol of BphF, 1.2 nmol of BphG, 2.4 nmol of BphAE, 400 nmol of NADH, and 500 nmol of the substrate (22). The metabolites were extracted at neutral pH with ethyl acetate and reacted with *n*-butylboronate (*n*BuB) for gas chromatography-time of flight mass spectrometry (GC-TOF-MS) analysis using previously reported protocols (33). The identity of each hydroxylated metabolite was determined based on chromatographic data reported previously by Viger et al. (31). Catalytic activities were assessed by monitoring metabolite production after 30 min of incubation. GC-MS peak areas were used to quantify substrate depletion and metabolite production. GC-TOF-MS analyses were performed using an HP7890A-series gas chromatograph (Agilent Technologies) using Pegasus BT (Leco).

Whole-cell assays to determine the potency of PCB degradation by various *E. coli*(pET14b-[*bphAE*]) strains. *E. coli* DH11S(pQE31[LB400-*bphFG*]/pET14b[*bphAE*]) cells expressing variant BphAEs were used to determine the ability of each BPDO to degrade a mixture of 11 PCBs using a protocol identical to the one reported previously by Barriault and Sylvestre (29) (see Table S2 in the supplemental material).

Modeling, docking, and structure analysis. The structures of S283M, p4-S283M, and RR41-S283M BphAEs were modeled by using SWISS-MODEL structural modeling software (<https://swissmodel.expasy.org/interactive>). The crystal structures of BphAE_{LB400} (RCBS PDB accession number 2XRX), BphAE_{p4} (RCBS PDB accession number 2XSH), and BphAE_{RR41} (RCBS PDB accession number 2YFJ) were chosen as the templates. The six structures of BphAE as protein targets were prepared using previously described methods (26). In the case of BphAE_{LB400} and its variants, the structural coordinates of dimer AB were used for docking. The ligands 2,2'-CB and 2,6'-CB were download as SDF files from PubChem (<http://pubchem.ncbi.nlm.nih.gov>) and converted into PDB format in Discover Studio. Both proteins and ligands were processed with AutoDockTools to obtain their proper PDBQT formats. The searching space for the ligand was centered on the mononuclear iron and contained 18 Å in each *x*, *y*, and *z* direction. AutoDock 1.5.6 (65) with default parameters was used to perform automatic docking (18).

SUPPLEMENTAL MATERIAL

Supplemental material is available online only.

SUPPLEMENTAL FILE 1, PDF file, 0.4 MB.

ACKNOWLEDGMENTS

We thank Marie-Eve Rivard and Thi Thanh My Pham for excellent technical support, Guiting Sun for her kind help in metabolite analysis, Monica Sharma for her help in structure analysis, and Pravindra Kumar for reading the manuscript and for discussions.

We declare that we have no conflicts of interest with the contents of this article.

This work was supported by the National Natural Science Foundation of China (41576165), the Foreword Key Priority Research Program of the Chinese Academy of Sciences (QYZDB-SSW-DQC013), the External Cooperation Program of the Chinese Academy of Sciences (133337KYSB20180015), and the Key Research Project of Frontier Science of the Chinese Academy of Sciences (QYZDB-SSW-DQC041).

REFERENCES

- Arensdorf JJ, Focht DD. 1995. A meta cleavage pathway for 4-chlorobenzoate, an intermediate in the metabolism of 4-chlorobiphenyl by *Pseudomonas cepacia* P166. *Appl Environ Microbiol* 61:443–447. <https://doi.org/10.1128/AEM.61.2.443-447.1995>.
- Bedard DL. 2003. Polychlorinated biphenyls in aquatic sediments: environmental fate and outlook for biological treatment, p 443–465. In Häggblom MM, Bossert ID (ed), *Dehalogenation: microbial processes and environmental applications*. Springer, Boston, MA.
- Passatore L, Rossetti S, Juwarkar AA, Massacci A. 2014. Phytoremediation and bioremediation of polychlorinated biphenyls (PCBs): state of knowledge and research perspectives. *J Hazard Mater* 278:189–202. <https://doi.org/10.1016/j.jhazmat.2014.05.051>.
- Sharma JK, Gautam RK, Nanekar SV, Weber R, Singh BK, Singh SK, Juwarkar AA. 2018. Advances and perspective in bioremediation of polychlorinated biphenyl-contaminated soils. *Environ Sci Pollut Res Int* 25:16355–16375. <https://doi.org/10.1007/s11356-017-8995-4>.
- Pieper DH. 2005. Aerobic degradation of polychlorinated biphenyls. *Appl Microbiol Biotechnol* 67:170–191. <https://doi.org/10.1007/s00253-004-1810-4>.
- Field JA, Sierra-Alvarez R. 2008. Microbial transformation and degradation of polychlorinated biphenyls. *Environ Pollut* 155:1–12. <https://doi.org/10.1016/j.envpol.2007.10.016>.
- Faroon OM, Samuel Keith L, Smith-Simon C, De Rosa CT, World Health Organization. 2003. Polychlorinated biphenyls: human health aspects. World Health Organization, Geneva, Switzerland.
- Mayes BA, McConnell EE, Neal BH, Brunner MJ, Hamilton SB, Sullivan TM, Peters AC, Ryan MJ, Toft JD, Singer AW, Brown JF, Menton RG, Moore JA. 1998. Comparative carcinogenicity in Sprague-Dawley rats of the polychlorinated biphenyl mixtures Aroclors 1016, 1242, 1254, and 1260. *Toxicol Sci* 41:62–76. <https://doi.org/10.1093/toxsci/41.1.62>.
- Aoki Y. 2001. Polychlorinated biphenyls, polychlorinated dibenzo-p-dioxins, and polychlorinated dibenzofurans as endocrine disruptors—what we have learned from Yusho disease. *Environ Res* 86:2–11. <https://doi.org/10.1006/enrs.2001.4244>.
- Ross G. 2004. The public health implications of polychlorinated biphenyls (PCBs) in the environment. *Ecotoxicol Environ Saf* 59:275–291. <https://doi.org/10.1016/j.ecoenv.2004.06.003>.
- Sylvestre M. 2004. Genetically modified organisms to remediate polychlorinated biphenyls. Where do we stand? *Int Biodeterior Biodegradation* 54:153–162. <https://doi.org/10.1016/j.ibiod.2004.03.011>.
- Lauby-Secretan B, Loomis D, Grosse Y, El Ghissassi F, Bouvard V, Benbrahim-Tallaa L, Guha N, Baan R, Mattock H, Straif K, WHO International Agency for Research on Cancer. 2013. Carcinogenicity of polychlorinated biphenyls and polybrominated biphenyls. *Lancet Oncol* 14:287–288. [https://doi.org/10.1016/S1470-2045\(13\)70104-9](https://doi.org/10.1016/S1470-2045(13)70104-9).
- Faroon OM, Keith S, Jones D, de Rosa C. 2001. Effects of polychlorinated biphenyls on development and reproduction. *Toxicol Ind Health* 17:63–93. <https://doi.org/10.1191/0748233701th0970a>.
- Meggo RE, Schnoor JL. 2013. Cleaning polychlorinated biphenyl (PCB)

- contaminated garden soil by phytoremediation. *Environ Sci (Ruse)* 1:33–52. <https://doi.org/10.12988/es.2013.13004>.
15. Witzig R, Junca H, Hecht HJ, Pieper DH. 2006. Assessment of toluene/biphenyl dioxygenase gene diversity in benzene-polluted soils: links between benzene biodegradation and genes similar to those encoding isopropylbenzene dioxygenases. *Appl Environ Microbiol* 72:3504–3514. <https://doi.org/10.1128/AEM.72.5.3504-3514.2006>.
 16. Vézina J, Barriault D, Sylvestre M. 2008. Diversity of the C-terminal portion of the biphenyl dioxygenase large subunit. *J Mol Microbiol Biotechnol* 15:139–151. <https://doi.org/10.1159/000121326>.
 17. Kagami O, Shindo K, Kyojima A, Takeda K, Ikenaga H, Furukawa K, Misawa N. 2008. Protein engineering on biphenyl dioxygenase for conferring activity to convert 7-hydroxyflavone and 5,7-dihydroxyflavone (chrysin). *J Biosci Bioeng* 106:121–127. <https://doi.org/10.1263/jbb.106.121>.
 18. Pham TT, Tu Y, Sylvestre M. 2012. Remarkable ability of *Pandoraea pnomenusa* B356 biphenyl dioxygenase to metabolize simple flavonoids. *Appl Environ Microbiol* 78:3560–3570. <https://doi.org/10.1128/AEM.00225-12>.
 19. Furukawa K, Suenaga H, Goto M. 2004. Biphenyl dioxygenases: functional versatility and directed evolution. *J Bacteriol* 186:5189–5196. <https://doi.org/10.1128/JB.186.16.5189-5196.2004>.
 20. Haddock JD, Gibson DT. 1995. Purification and characterization of the oxygenase component of biphenyl 2,3-dioxygenase from *Pseudomonas* sp. strain LB400. *J Bacteriol* 177:5834–5839. <https://doi.org/10.1128/jb.177.20.5834-5839.1995>.
 21. Hurtubise Y, Barriault D, Powlowski J, Sylvestre M. 1995. Purification and characterization of the *Comamonas testosteroni* B-356 biphenyl dioxygenase components. *J Bacteriol* 177:6610–6618. <https://doi.org/10.1128/jb.177.22.6610-6618.1995>.
 22. Hurtubise Y, Barriault D, Sylvestre M. 1996. Characterization of active recombinant His-tagged oxygenase component of *Comamonas testosteroni* B-356 biphenyl dioxygenase. *J Biol Chem* 271:8152–8156. <https://doi.org/10.1074/jbc.271.14.8152>.
 23. Brühlmann F, Chen W. 1999. Tuning biphenyl dioxygenase for extended substrate specificity. *Biotechnol Bioeng* 63:544–551. [https://doi.org/10.1002/\(SICI\)1097-0290\(19990605\)63:5<544::AID-BIT4>3.0.CO;2-6](https://doi.org/10.1002/(SICI)1097-0290(19990605)63:5<544::AID-BIT4>3.0.CO;2-6).
 24. Kumamaru T, Suenaga H, Mitsuoka M, Watanabe T, Furukawa K. 1998. Enhanced degradation of polychlorinated biphenyls by directed evolution of biphenyl dioxygenase. *Nat Biotechnol* 16:663–666. <https://doi.org/10.1038/nbt0798-663>.
 25. Zielinski M, Kahl S, Standfuss-Gabisch C, Camara B, Seeger M, Hofer B. 2006. Generation of novel-substrate-accepting biphenyl dioxygenases through segmental random mutagenesis and identification of residues involved in enzyme specificity. *Appl Environ Microbiol* 72:2191–2199. <https://doi.org/10.1128/AEM.72.3.2191-2199.2006>.
 26. Dhindwal S, Gomez-Gil L, Neau DB, Pham TT, Sylvestre M, Eltis LD, Bolin JT, Kumar P. 2016. Structural basis of the enhanced pollutant-degrading capabilities of an engineered biphenyl dioxygenase. *J Bacteriol* 198:1499–1512. <https://doi.org/10.1128/JB.00952-15>.
 27. Mondello FJ, Turcich MP, Lobos JH, Erickson BD. 1997. Identification and modification of biphenyl dioxygenase sequences that determine the specificity of polychlorinated biphenyl degradation. *Appl Environ Microbiol* 63:3096–3103. <https://doi.org/10.1128/AEM.63.8.3096-3103.1997>.
 28. Barriault D, Lépine F, Mohammadi M, Milot S, Leberre N, Sylvestre M. 2004. Revisiting the regiospecificity of *Burkholderia xenovorans* LB400 biphenyl dioxygenase toward 2,2'-dichlorobiphenyl and 2,3,2',3'-tetrachlorobiphenyl. *J Biol Chem* 279:47489–47496. <https://doi.org/10.1074/jbc.M406808200>.
 29. Barriault D, Sylvestre M. 2004. Evolution of the biphenyl dioxygenase BphA from *Burkholderia xenovorans* LB400 by random mutagenesis of multiple sites in region III. *J Biol Chem* 279:47480–47488. <https://doi.org/10.1074/jbc.M406805200>.
 30. Mohammadi M, Sylvestre M. 2005. Evolving the profile of metabolites generated during oxidation of dibenzofuran and chlorodibenzofurans by the biphenyl catabolic pathway enzymes. *Chem Biol* 12:835–846. <https://doi.org/10.1016/j.chembiol.2005.05.017>.
 31. Viger JF, Mohammadi M, Barriault D, Sylvestre M. 2012. Metabolism of chlorobiphenyls by a variant biphenyl dioxygenase exhibiting enhanced activity toward dibenzofuran. *Biochem Biophys Res Commun* 419:362–367. <https://doi.org/10.1016/j.bbrc.2012.02.029>.
 32. Kumar P, Mohammadi M, Viger JF, Barriault D, Gomez-Gil L, Eltis LD, Bolin JT, Sylvestre M. 2011. Structural insight into the expanded PCB-degrading abilities of a biphenyl dioxygenase obtained by directed evolution. *J Mol Biol* 405:531–547. <https://doi.org/10.1016/j.jmb.2010.11.009>.
 33. Mohammadi M, Viger JF, Kumar P, Barriault D, Bolin JT, Sylvestre M. 2011. Retuning Rieske-type oxygenases to expand substrate range. *J Biol Chem* 286:27612–27621. <https://doi.org/10.1074/jbc.M111.255174>.
 34. Dhindwal S, Patil DN, Mohammadi M, Sylvestre M, Tomar S, Kumar P. 2011. Biochemical studies and ligand-bound structures of biphenyl dehydrogenase from *Pandoraea pnomenusa* strain B-356 reveal a basis for broad specificity of the enzyme. *J Biol Chem* 286:37011–37022. <https://doi.org/10.1074/jbc.M111.291013>.
 35. Hurtubise Y, Barriault D, Sylvestre M. 1998. Involvement of the terminal oxygenase β subunit in the biphenyl dioxygenase reactivity pattern toward chlorobiphenyls. *J Bacteriol* 180:5828–5835. <https://doi.org/10.1128/JB.180.22.5828-5835.1998>.
 36. Gomez-Gil L, Kumar P, Barriault D, Bolin JT, Sylvestre M, Eltis LD. 2007. Characterization of biphenyl dioxygenase of *Pandoraea pnomenusa* B-356 as a potent polychlorinated biphenyl-degrading enzyme. *J Bacteriol* 189:5705–5715. <https://doi.org/10.1128/JB.01476-06>.
 37. Arnett CM, Perales JV, Haddock JD. 2000. Influence of chlorine substituents on rates of oxidation of chlorinated biphenyls by the biphenyl dioxygenase of *Burkholderia* sp. strain LB400. *Appl Environ Microbiol* 66:2928–2933. <https://doi.org/10.1128/aem.66.7.2928-2933.2000>.
 38. Sylvestre M. 2013. Prospects for using combined engineered bacterial enzymes and plant systems to rhizoremediate polychlorinated biphenyls. *Environ Microbiol* 15:907–915. <https://doi.org/10.1111/1462-2920.12007>.
 39. Boyd DR, Bugg TD. 2006. Arene cis-dihydrodiol formation: from biology to application. *Org Biomol Chem* 4:181–192. <https://doi.org/10.1039/b513226f>.
 40. Seo J, Kang SI, Ryu JY, Lee YJ, Park KD, Kim M, Won D, Park HY, Ahn JH, Chong Y, Kanaly RA, Han J, Hur HG. 2010. Location of flavone B-ring controls regioselectivity and stereoselectivity of naphthalene dioxygenase from *Pseudomonas* sp. strain NCIB 9816-4. *Appl Microbiol Biotechnol* 86:1451–1462. <https://doi.org/10.1007/s00253-009-2389-6>.
 41. Vézina J, Barriault D, Sylvestre M. 2007. Family shuffling of soil DNA to change the regiospecificity of *Burkholderia xenovorans* LB400 biphenyl dioxygenase. *J Bacteriol* 189:779–788. <https://doi.org/10.1128/JB.01267-06>.
 42. Erickson BD, Mondello FJ. 1993. Enhanced biodegradation of polychlorinated biphenyls after site-directed mutagenesis of a biphenyl dioxygenase gene. *Appl Environ Microbiol* 59:3858–3862. <https://doi.org/10.1128/AEM.59.11.3858-3862.1993>.
 43. Beil S, Mason JR, Timmis KN, Pieper DH. 1998. Identification of chlorobenzene dioxygenase sequence elements involved in dechlorination of 1,2,4,5-tetrachlorobenzene. *J Bacteriol* 180:5520–5528. <https://doi.org/10.1128/JB.180.21.5520-5528.1998>.
 44. Perales RE, Resnick SM, Yu CL, Boyd DR, Sharma ND, Gibson DT. 2000. Regioselectivity and enantioselectivity of naphthalene dioxygenase during arene cis-dihydroxylation: control by phenylalanine 352 in the alpha subunit. *J Bacteriol* 182:5495–5504. <https://doi.org/10.1128/jb.182.19.5495-5504.2000>.
 45. Zielinski M, Backhaus S, Hofer B. 2002. The principal determinants for the structure of the substrate-binding pocket are located within a central core of a biphenyl dioxygenase α subunit. *Microbiology* 148:2439–2448. <https://doi.org/10.1099/00221287-148-8-2439>.
 46. Wang Y, Li J, Liu AJ. 2017. Oxygen activation by mononuclear nonheme iron dioxygenases involved in the degradation of aromatics. *J Biol Inorg Chem* 22:395–405. <https://doi.org/10.1007/s00775-017-1436-5>.
 47. Kumar P, Mohammadi M, Dhindwal S, Pham TT, Bolin JT, Sylvestre M. 2012. Structural insights into the metabolism of 2-chlorodibenzofuran by an evolved biphenyl dioxygenase. *Biochem Biophys Res Commun* 421:757–762. <https://doi.org/10.1016/j.bbrc.2012.04.078>.
 48. Dong X, Fushinobu S, Fukuda E, Terada T, Nakamura S, Shimizu K, Nojiri H, Omori T, Shoun H, Wakagi T. 2005. Crystal structure of the terminal oxygenase component of cumene dioxygenase from *Pseudomonas fluorescens* IP01. *J Bacteriol* 187:2483–2490. <https://doi.org/10.1128/JB.187.7.2483-2490.2005>.
 49. Hirose J, Suyama A, Hayashida S, Furukawa K. 1994. Construction of hybrid biphenyl (bph) and toluene (tod) genes for functional analysis of aromatic ring dioxygenases. *Gene* 138:27–33. [https://doi.org/10.1016/0378-1119\(94\)90779-x](https://doi.org/10.1016/0378-1119(94)90779-x).
 50. Zielinski M, Kahl S, Hecht HJ, Hofer B. 2003. Pinpointing biphenyl dioxygenase residues that are crucial for substrate interaction. *J Bacteriol* 185:6976–6980. <https://doi.org/10.1128/jb.185.23.6976-6980.2003>.

51. Teng Y, Wang X, Li L, Li Z, Luo Y. 2015. Rhizobia and their bio-partners as novel drivers for functional remediation in contaminated soils. *Front Plant Sci* 6:32. <https://doi.org/10.3389/fpls.2015.00032>.
52. Wang X, Teng Y, Luo Y, Dick RP. 2016. Biodegradation of 3,3',4,4'-tetrachlorobiphenyl by *Sinorhizobium meliloti* NM. *Bioresour Technol* 201:261–268. <https://doi.org/10.1016/j.biortech.2015.11.056>.
53. Goto E, Haga Y, Kubo M, Itoh T, Kasai C, Shoji O, Yamamoto K, Matsumura C, Nakano T, Inui H. 2018. Metabolic enhancement of 2,3',4,4',5-pentachlorobiphenyl (CB118) using cytochrome P450 monooxygenase isolated from soil bacterium under the presence of perfluorocarboxylic acids (PFCAs) and the structural basis of its metabolism. *Chemosphere* 210:376–383. <https://doi.org/10.1016/j.chemosphere.2018.07.026>.
54. Suenaga H, Goto M, Furukawa K. 2006. Active-site engineering of biphenyl dioxygenase: effect of substituted amino acids on substrate specificity and regiospecificity. *Appl Microbiol Biotechnol* 71: 168–176. <https://doi.org/10.1007/s00253-005-0135-2>.
55. Suenaga H, Watanabe T, Sato M, Ngadiman, Furukawa K. 2002. Alteration of regiospecificity in biphenyl dioxygenase by active-site engineering. *J Bacteriol* 184:3682–3688. <https://doi.org/10.1128/jb.184.13.3682-3688.2002>.
56. Feng T, Lin H, Tang J, Feng Y. 2014. Characterization of polycyclic aromatic hydrocarbons degradation and arsenate reduction by a versatile *Pseudomonas* isolate. *Int Biodeterior Biodegradation* 90:79–87. <https://doi.org/10.1016/j.ibiod.2014.01.015>.
57. Singh P, Singh SM, Dhakephalkar P. 2014. Diversity, cold active enzymes and adaptation strategies of bacteria inhabiting glacier cryoconite holes of High Arctic. *Extremophiles* 18:229–242. <https://doi.org/10.1007/s00792-013-0609-6>.
58. Weiland-Bräuer N, Fischer MA, Schramm K-W, Schmitz RA. 2017. Polychlorinated biphenyl (PCB)-degrading potential of microbes present in a cryoconite of Jamtalferner glacier. *Front Microbiol* 8:1105. <https://doi.org/10.3389/fmicb.2017.01105>.
59. Su X, Li S, Cai J, Xiao Y, Tao L, Hashmi MZ, Lin H, Chen J, Mei R, Sun F. 2019. Aerobic degradation of 3,3',4,4'-tetrachlorobiphenyl by a resuscitated strain *Castellaniella* sp. SPC4: kinetics model and pathway for biodegradation. *Sci Total Environ* 688:917–925. <https://doi.org/10.1016/j.scitotenv.2019.06.364>.
60. Erickson BD, Mondello FJ. 1992. Nucleotide sequencing and transcriptional mapping of the genes encoding biphenyl dioxygenase, a multi-component polychlorinated-biphenyl-degrading enzyme in *Pseudomonas* strain LB400. *J Bacteriol* 174:2903–2912. <https://doi.org/10.1128/jb.174.9.2903-2912.1992>.
61. Miroux B, Walker JE. 1996. Over-production of proteins in *Escherichia coli*: mutant hosts that allow synthesis of some membrane proteins and globular proteins at high levels. *J Mol Biol* 260:289–298. <https://doi.org/10.1006/jmbi.1996.0399>.
62. Barriault D, Plante MM, Sylvestre M. 2002. Family shuffling of a targeted *bphA* region to engineer biphenyl dioxygenase. *J Bacteriol* 184:3794–3800. <https://doi.org/10.1128/jb.184.14.3794-3800.2002>.
63. Laemmli UK. 1970. Cleavage of structural proteins during the assembly of the head of bacteriophage T₄. *Nature* 227:680–685. <https://doi.org/10.1038/227680a0>.
64. Imbeault NY, Powlowski JB, Colbert CL, Bolin JT, Eltis LD. 2000. Steady-state kinetic characterization and crystallization of a polychlorinated biphenyl-transforming dioxygenase. *J Biol Chem* 275:12430–12437. <https://doi.org/10.1074/jbc.275.17.12430>.
65. Morris GM, Huey R, Lindstrom W, Sanner MF, Belew RK, Goodsell DS, Olson AJ. 2009. AutoDock4 and AutoDockTools4: automated docking with selective receptor flexibility. *J Comput Chem* 30:2785–2791. <https://doi.org/10.1002/jcc.21256>.
66. L'Abbée JB, Tu Y, Barriault D, Sylvestre M. 2011. Insight into the metabolism of 1,1,1-trichloro-2,2-bis(4-chlorophenyl)ethane (DDT) by biphenyl dioxygenases. *Arch Biochem Biophys* 516:35–44. <https://doi.org/10.1016/j.abb.2011.09.016>.